Supplemental information for:

Integrative x-ray structure and molecular modeling for the rationalization of procaspase-8 inhibitor potency and selectivity

Janice H. Xu[1,2], Jerome Eberhardt[2], Brianna Hill-Payne[4], Gonzalo E. González-Páez[1,2], José Omar Castellón[4], Benjamin F. Cravatt[3], Stefano Forli[2*], Dennis W. Wolan[1,2*], Keriann M. Backus[4*]

[1] Department of Molecular Medicine, [2] Department of Structural and Computational Biology, [3] Department of Chemistry, The Scripps Research Institute, 10550 North Torrey Pines Road, La Jolla, CA 92037
[4] Departments of Biological Chemistry and Chemistry and Biochemistry, David Geffen School of Medicine, University of California, Los Angeles, 405 Hilgard Avenue, Los Angeles, CA 90095

*Corresponding Authors: forli@scripps.edu, wolan@scripps.edu, and kbackus@mednet.ucla.edu

Table of Contents

Table S1. X-ray data collection and structure refinement statistics of procaspase-8 in complex with **63-*R***.

Structure	6PX9
Space group	P 3_1
Cell dimensions	
a, b, c; Å	101.3, 101.3, 175.5
α, β, γ; º	90, 90, 120
Data Processing	
Resolution, Å (outer shell)	50.0-2.88 (2.93-2.88)
Completeness, %	99.5 (99.5)
Unique reflections	45,476 (2,243)
Redundancy	4.5 (4.4)
R_{meas} (%)[a]	33.6 (150)
R_{merge} (%)[b]	29.7 (132)
$R_{p.i.m.}$ (%)[c]	15.6 (70.5)
Average I / Average σ (I)	8.1 (1.7)
$CC_{1/2}$	67.9 (17.4)
Refinement	
Resolution, Å (outer shell)	50.0-2.88 (2.94-2.88)
No. reflections (test set)[d]	45,343 (2,253)
R_{cryst} (%)[e]	28.9 (44.2)
R_{free} (%)	36.6 (49.4)
Protein atoms / Waters	9,845 / 4 / 30
CV coordinate error (Å)[f]	0.90
RMSD bonds (Å) / angles º	0.003 / 0.677
B-values protein/waters/ligands (Å^2)	44 / 39 / 43
Ramachandran Statistics (%)	
Preferred	89.2
Allowed	10.8
Outliers	0

[a]$R_{meas} = \{\Sigma_{hkl}[N/(N-1)]1/2\Sigma_i|I_{i(hkl)} - \langle I_{(hkl)}\rangle|\} / \Sigma_{hkl}\Sigma_i I_{i(hkl)}$, where $I_{i(hkl)}$ are the observed intensities, $\langle I_{(hkl)}\rangle$ are the average intensities and N is the multiplicity of reflection hkl. [b]$R_{merge} = \Sigma_{hkl}\Sigma_i|I_{i(hkl)} - \langle I_{(hkl)}\rangle| / \Sigma_{hkl}\Sigma_i I_{i(hkl)}$ where $I_{i(hkl)}$ is the i^{th} measurement of reflection h and $\langle I_{(hkl)}\rangle$ is the average measurement value. [c]$R_{p.i.m.}$ (precision-indicating R_{merge}) $= \Sigma_{hkl}[1/(N_{hkl} - 1)]^{1/2}\Sigma_i|I_{i(hkl)} - \langle I_{(hkl)}\rangle|/\Sigma_{hkl}\Sigma_i I_{i(hkl)}$. [d]Reflections with I > 0 were used for refinement.[1-3] [e]$R_{cryst} = \Sigma_h||F_{obs}|-|F_{calc}||/\Sigma|F_{obs}|$, where F_{obs} and F_{calc} are the calculated and observed structure factor amplitudes, respectively. R_{free} is R_{cryst} with 5.0% test set structure factors. [f]Cross-validated (CV) Luzzati coordinate errors.

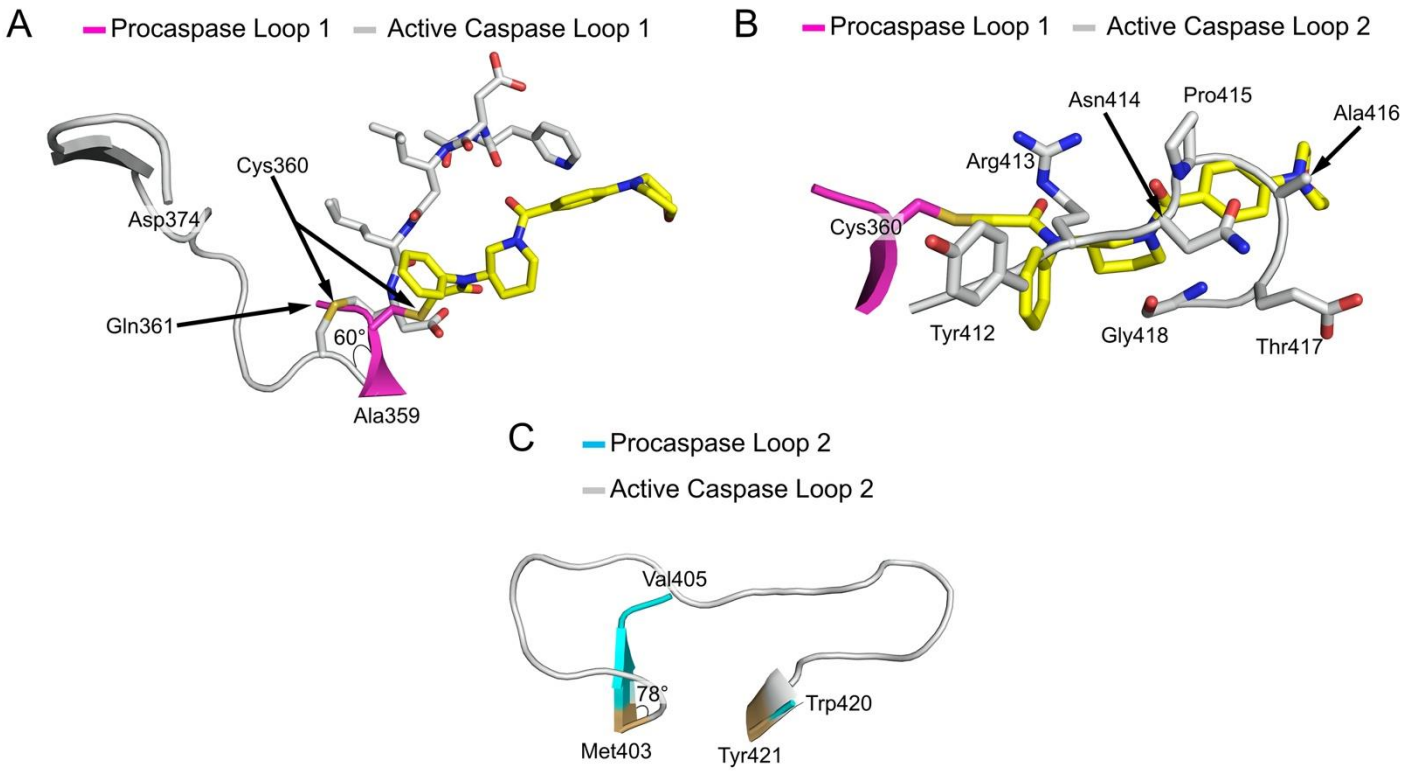

Fig. S1. Overlay of pro- and active caspase-8 loops 1 and 2. (A) Cartoon representation of the N-terminal end of loop 1 where the catalytic Cys360 of active caspase-8 repositions 60° from Cys360 in the procaspase-8 structure (carbons are magenta, grey, yellow, and green for procaspase-8, active caspase-8, **63-*R***, and active caspase-8 peptide inhibitor respectively, with blue nitrogens, and red oxygens). (B) Active caspase residues 412-417 from loop 1 directly superimpose over the position of **63-*R***. (C) Cartoon representation of loop 2 where procaspase-8 is cyan and active caspase-8 is grey. Met403 is shifted 78° in the activated caspase-8, changing the secondary structure of loop 2 from the β-sheet seen in procaspase-8 into a disordered loop.

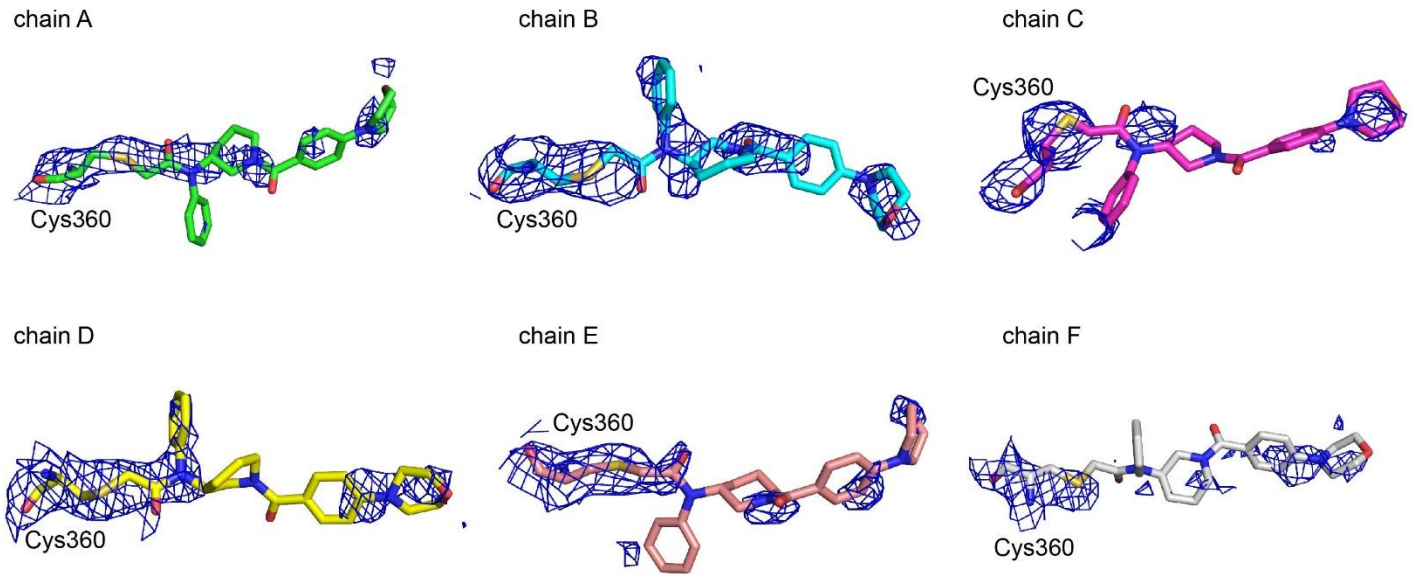

Fig. S2. Simulated-annealing omit map density contoured at 1.0σ of catalytic Cys360 bound to inhibitor **63-*R*** in all 6 subunits. Atoms colored as Supplementary Fig. 1.

Table S2. Modification of procaspase-8 crystals by **63-*R*.** Crystals from procaspase-8 co-crystallized with **63-*R*** were harvested, reduced, alkylated, subjected to trypsin digest and analyzed by LC-MS/MS. Underline marks the **63-*R***-modified cysteine.

Protein	Cysteine	Fragment #	Peptide	M+H calculated (m/z)	M+H observed (m/z)	Charge
CASP8	C360	63-*R*	K.VFFIQAC<u>Q</u>GDNYQK.G	1034.99	1034.99	+2

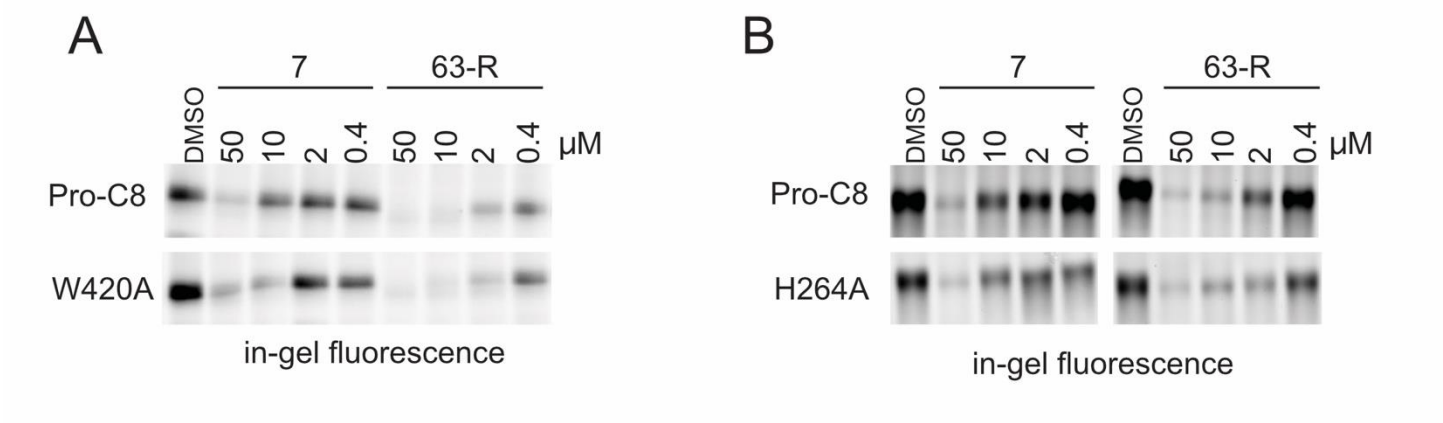

Fig. S3. Competitive ABPP gels of the W420A and H264A mutated forms of procaspase-8. (A) Recombinant procaspase-8 (D384A and D394A), and mutant procaspase-8 proteins (W420A) were added to HEK 293T soluble lysates to a final protein concentration of 500 nM. The protein-containing lysates were then treated with **7** or **63-*R*** at the indicated concentrations or vehicle (DMSO) for 1h, followed by labeling with **61** (10 μM) for 1h, "click" conjugation to rhodamine-azide, and analysis by SDS-PAGE and in-gel fluorescence. (B) As in 'A' but with the H264A mutant of procaspase-8. Due to observed instability of the H264A protein upon multiple freeze thaw cycles, the protein was assayed in *E coli* lysates after overexpression without freezing and without further purification.

A

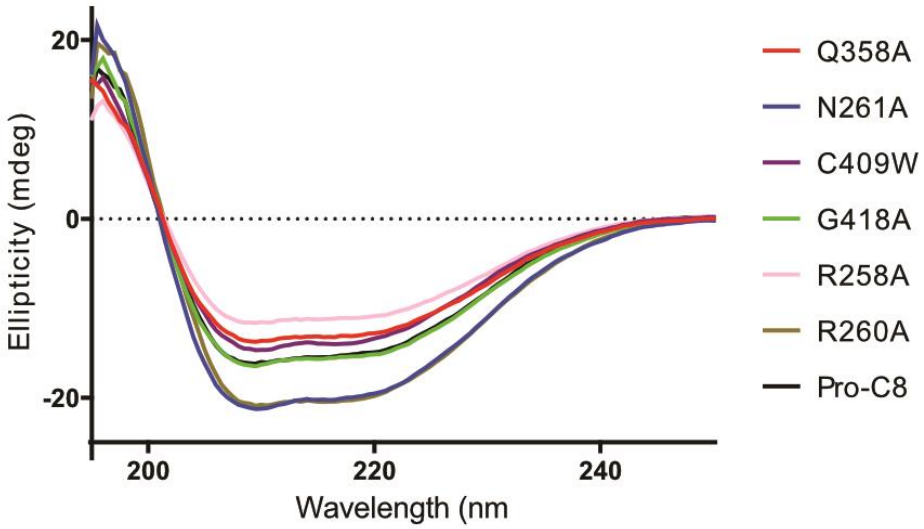

	Alpha Helix	Beta Sheet	Turn	Other
Pro-C8	15.9%	38.3%	13.9%	33.4%
R260A	15.3%	42.5%	14.9%	29.3%
Q358A	15.0%	42.5%	13.9%	30.6%
G418A	15.1%	38.5%	11.1%	36.5%
C409W	14.6%	40.2%	12.0%	34.0%
R258A	15.9%	36.9%	13.5%	34.8%
N261A	15.4%	42.5%	13.4%	30.1%

B

Fig. S4. (A) Circular dichroism spectra and calculated secondary structures of caspase-8 mutant proteins. (B) Relative abundance of the indicated recombinant procaspase-8 constructs was visualized by Western blot with an anti-his antibody.

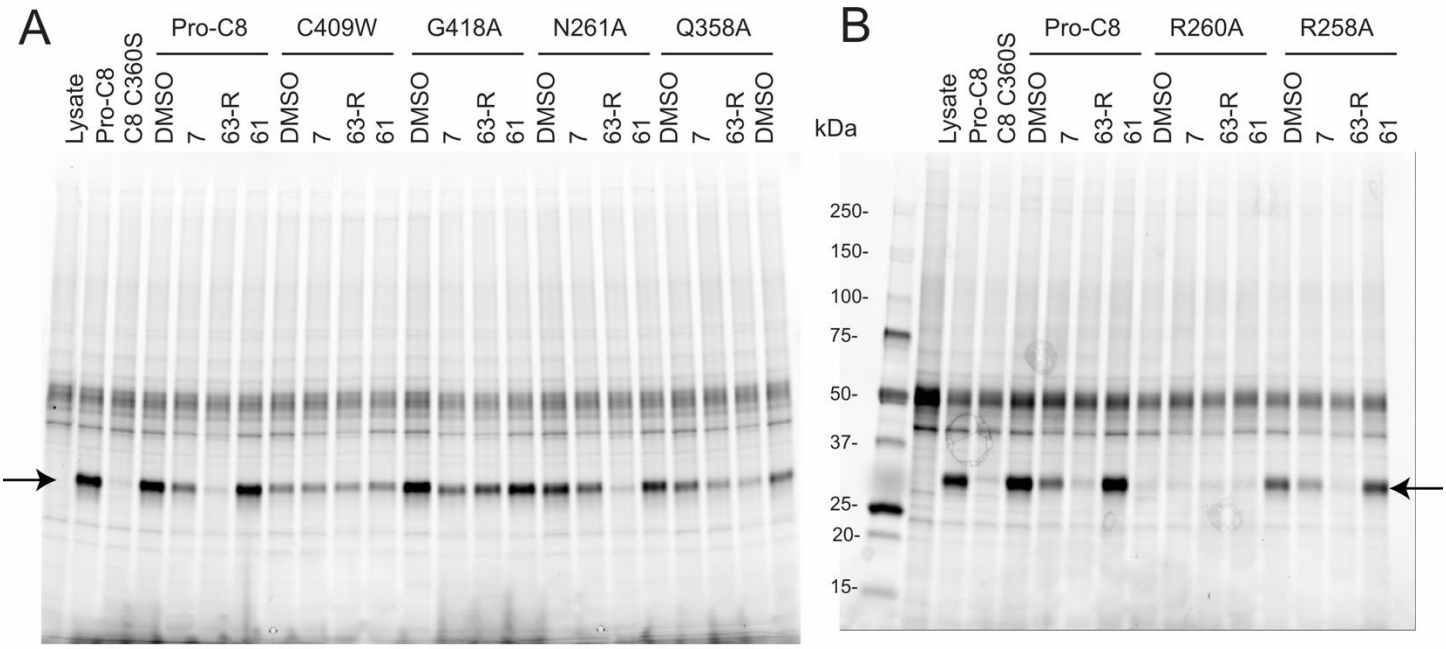

Fig. S5. Representative full-length gels for single dose competitive labeling experiments quantified in Fig. 5B-I. (A) Recombinant procaspase-8 (D384A and D394A), and mutant procaspase-8 proteins (C409W, G418A, N261A, or Q358A) were added to HEK 293T soluble lysates to a final protein concentration of 500 nM. The protein-containing lysates were then treated with **7**, **63-*R***, **62** (all at 10 μM), or vehicle (DMSO) for 1h, followed by labeling with **61** (10 μM) for 1h, "click" conjugation to rhodamine-azide, and analysis by SDS-PAGE and in-gel fluorescence. Note that the C360S-mutant of procaspase-8, which lacks the catalytic cysteine, did not label with **61**. (B) As in 'A' but with the R260A- and R258A-mutants of procaspase-8. Arrows indicate procaspase-8 band.

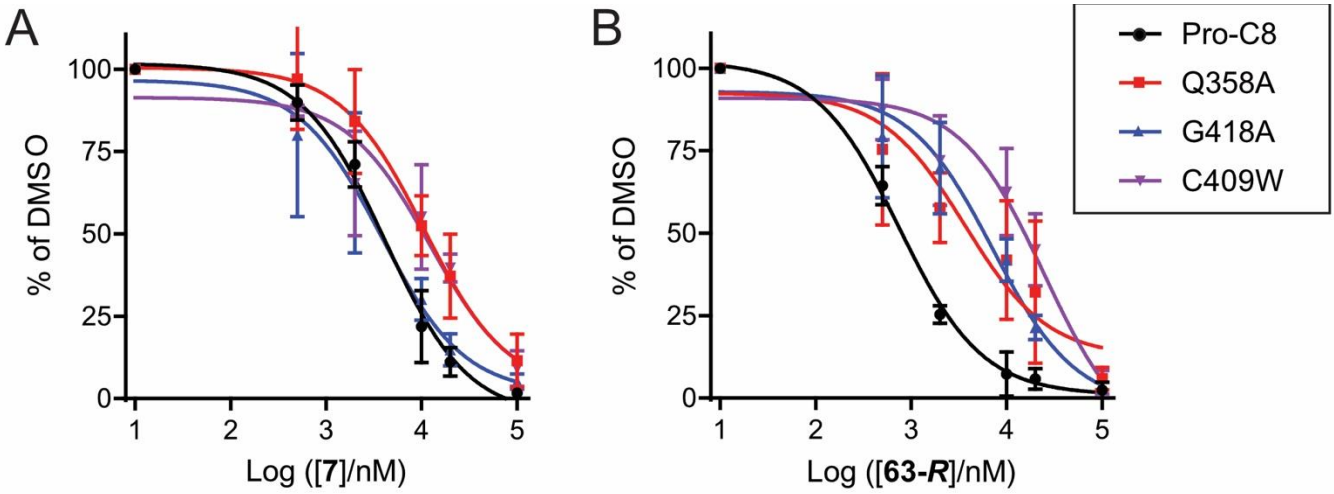

C

	Pro-C8		C409W		G418A		Q358A	
Compound	**7**	**63-*R***	**7**	**63-*R***	**7**	**63-*R***	**7**	**63-*R***
Apparent IC_{50} (μM)	4.10	0.75	12.18	24.59	3.80	7.14	10.59	3.64
95% CI (μM)	2.94–5.80	0.62–0.94	3.37–32.80	10.53–63.83	1.55–9.13	3.12–14.70	5.15–20.85	0.63–24.98

Fig. S6. Site-directed mutagenesis studies to identify residues that determine compound binding to procaspase-8. (A and B) Apparent IC_{50} curves for blockade of **61** labeling of procaspase-8 (pro-C8) harboring the indicated mutations by pre-treatment with **7** (A) or **63-*R*** (B). (C) Calculated apparent IC_{50} values, including 95% confidence intervals derived from the three replicate experiments shown in A and B.

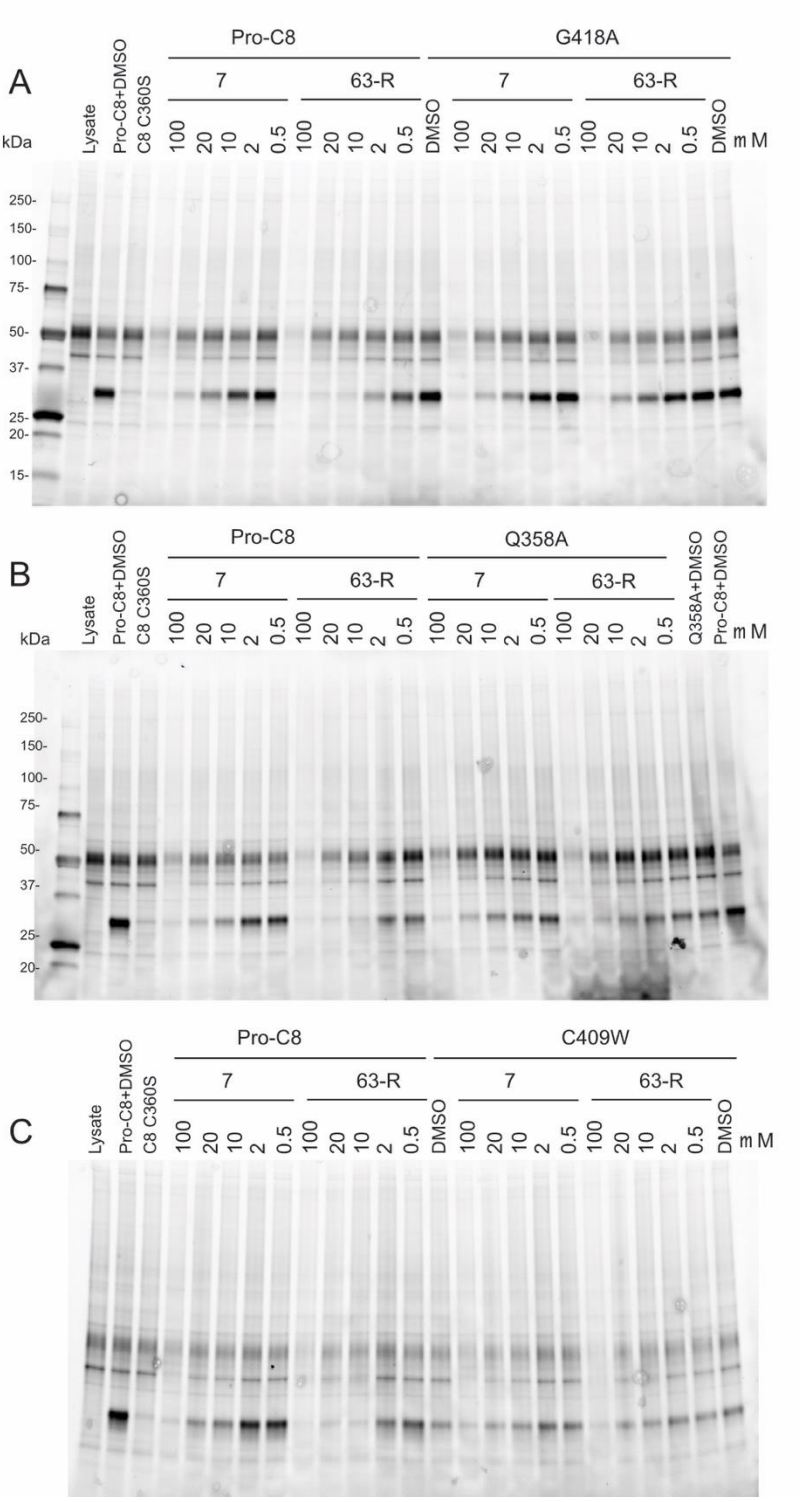

Fig. S7. Representative full-length gels for IC_{50} competitive labeling experiments quantified in Fig. 5J and Fig. 5 supplement 3. (A) Recombinant procaspase-8 (D384A and D394A), and C409W-mutant procaspase-8 were added to HEK 293T soluble lysates to a final protein concentration of 500 nM. The protein-containing lysates were then treated with **7**, **63-*R***, **62** at the indicated concentrations, or vehicle (DMSO) for 1h, followed by labeling with **61** (10 μM) for 1h, "click" conjugation to rhodamine-azide. (B) as in 'A', with Q358A-mutant pro-caspase-8. (C) as in 'A', with C409W-mutant procaspase-8.

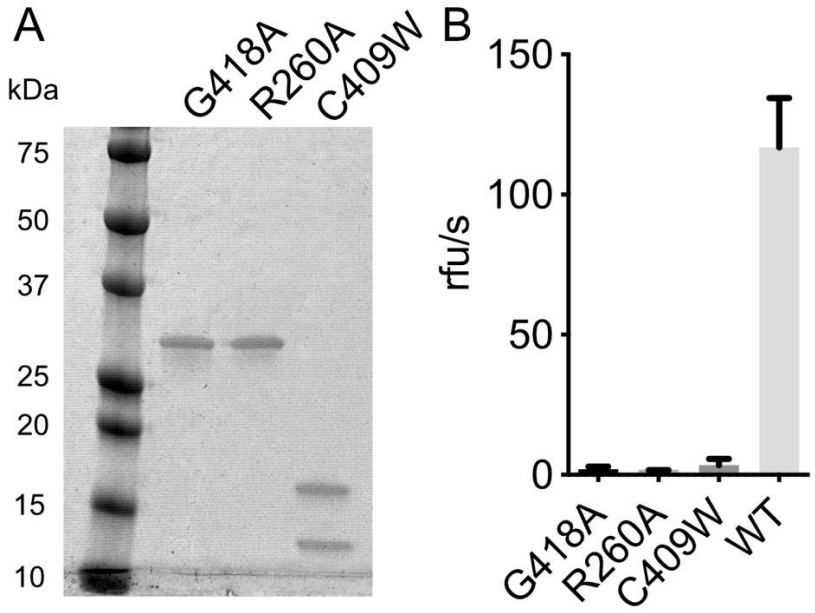

Fig. S8. (A) SDS-PAGE reducing gel of purified caspase-8 single point mutants G418A, R260A, and C409W. The mutation of Q358 to alanine did not produce stable protein. (B) Activity assay of G418A, R260A, and C409W caspase-8 mutants using Ac-IETD-AMAC as a substrate. The assay was performed as previously described.[4] Despite self-activation during overexpression in *E. coli*, C409W is inactive against the tetrapeptide substrate.

Supporting Information References

1. Weiss, M. S. (2001) Global indicators of X-ray data quality, *J. Appl. Crystallogr. 34*, 130-135.
2. Weiss, M. S., and Hilgenfeld, R. (1997) On the use of the merging R factor as a quality indicator for X-ray data, *J. Appl. Crystallogr. 30*, 203-205.
3. Karplus, P. A., and Diederichs, K. (2015) Assessing and maximizing data quality in macromolecular crystallography, *Curr. Opin. Struct. Biol. 34*, 60-68.
4. Solania, A., Gonzalez-Paez, G. E., and Wolan, D. W. (2019) Selective and rapid cell-permeable inhibitor of human caspase-3, *ACS Chem. Biol. 14*, 2463-2470.